Journal of Assisted Reproduction and Genetics (2021) 38:2581–2590
https://doi.org/10.1007/s10815-021-02282-2

REPRODUCTIVE PHYSIOLOGY AND DISEASE

Mitochondrial content, activity, and morphology in prepubertal and adult human ovaries

Rossella Masciangelo[1] · Maria Costanza Chiti[1] · Alessandra Camboni[1] · Christiani Andrade Amorim[1] · Jacques Donnez[2] · Marie-Madeleine Dolmans[1,3]

Received: 10 March 2021 / Accepted: 15 July 2021 / Published online: 31 July 2021

Abstract

Purpose To investigate whether mitochondrial content, activity, and morphology differ in prepubertal versus adult ovarian follicles.

Methods Ovarian tissue was collected from 7 prepubertal girls (age 1–10 years) and 6 adult women (age 20–35 years). Primordial and primary follicles were isolated from frozen-thawed prepubertal and adult ovarian tissue and their viability was assessed. Mitochondrial content was investigated by TOMM20 immunostaining of prepubertal and adult ovarian tissue, while mitochondrial activity in isolated follicles was analyzed by MitoTracker CM-H2XRos and JC-1. Frozen-thawed ovarian tissue from the same patients was also evaluated by transmission electron microscopy to examine mitochondrial morphology.

Results Higher TOMM20 staining was detected in prepubertal follicles compared to their adult counterparts, indicating the presence of more mitochondria in prepubertal follicles. Analysis of mitochondrial activity by MitoTracker showed higher fluorescence intensity in prepubertal follicles, suggesting that follicles in this group are more active than adult follicles. JC-1 analysis did not reveal any statistically significant difference in the inactive/active ratio between the two groups. Moreover, ultrastructural analysis by TEM detected morphological differences in the shape and cristae of prepubertal mitochondria, probably suggesting a mechanism of response to autophagy.

Conclusion Differences in the number, activity, and morphology of mitochondria were reported, suggesting that consequential modifications might occur during puberty, which could be the window of opportunity required by mitochondria to undergo changes needed to reach maturity, and hence the capacity for ovulation and fertilization.

Keywords Prepubertal ovarian tissue · Mitochondria · Follicle isolation · Transmission electron microscopy

Introduction

Recent advances in cancer treatment have led to improved survival rates in many cancer patients [1], but most still suffer the long-term side effects of chemotherapy and radiotherapy, notably premature ovarian insufficiency [1, 2]. Ovarian tissue cryopreservation and transplantation are currently the only available fertility preservation option for prepubertal patients [1]. However, while one live birth was recently obtained from ovarian tissue collected before puberty [3], literature on ovarian tissue from young girls remains scarce. Experimental studies have demonstrated the capacity of prepubertal follicles to grow to advanced stages [4–6], but adequate growth competence and maturity are still to be assessed. Several studies have evaluated the capability of oocytes to develop into viable embryos upon fertilization and most of them have identified the central role of mitochondria in this process [7]. Mitochondria are double-membrane-bound organelles ubiquitously present in the cytoplasm of eukaryotic cells and possess their own DNA (mtDNA). They generate most of the energy in cells in the form of adenosine triphosphate (ATP) through the process of oxidative phosphorylation. This process is possible thanks

✉ Marie-Madeleine Dolmans
marie-madeleine.dolmans@uclouvain.be

[1] Pôle de Recherche en Gynécologie, Institut de Recherche Expérimentale Et Clinique, Université Catholique de Louvain, Avenue Mounier 52, bte. B1.52.02, 1200 Brussels, Belgium

[2] Société de Recherche Pour L'Infertilité, Avenue Grandchamp 143, 1150 Brussels, Belgium

[3] Département de Gynécologie, Cliniques Universitaires St. Luc, Avenue Hippocrate 10, 1200 Brussels, Belgium

to generation of mitochondrial membrane potential ($\Delta\Psi m$), which is kept stable in order to ensure appropriate cell functioning and viability [8]. The role of mitochondria in determining the developmental capacity of mammalian oocytes is increasingly evident due to their function as energy providers [9], while their quantity and functionality are fundamental to the quality of oocytes and their fertilization and maturation [10]. Indeed, reduced efficiency of mitochondrial oxidative phosphorylation and ATP production in oocytes is related to poor embryo development [11–14].

It is widely known that mitochondria play a central role in ovarian aging through their major contribution to cell survival and apoptosis [9, 10, 14, 15], and that maternal age is associated with increased oxidative stress in oocytes, resulting in mitochondrial dysfunction [15]. However, published literature on mitochondrial function in prepubertal patients is limited [15]. The aim of this study was to evaluate mitochondrial content and activity in preantral follicles in prepubertal compared to adult ovarian tissue, in order to gain further insights into follicle characterization in prepubertal patients.

Material and methods

Experimental design

Use of human ovarian tissue was approved by the Institutional Review Board of the Université Catholique de Louvain, Brussels (Reference 2012/23MAR/125). Based on informed consent, cryopreserved ovarian tissue from deceased patients can be utilized for scientific purposes, so frozen-thawed human ovarian tissue was obtained from 7 deceased prepubertal patients (age 1–10 years, mean 5.1 years) for the study. All 7 patients had suffered from malignant diseases: Ewing sarcoma $n=1$, medulloblastoma $n=2$, sarcoma $n=3$, leukemia $n=1$. Cryopreservation was performed before cancer treatment in each case.

Frozen-thawed ovarian tissue from 6 adult women (age 20–35 years, mean 27.8 years) was used for controls. All 6 patients had undergone cryopreservation for cancer indications (breast cancer $n=3$, Hodgkin's lymphoma $n=2$, sarcoma $n=1$) and provided written informed consent to donate their cryopreserved ovarian tissue to research.

Ovarian tissue freezing and thawing

Cryopreservation of ovarian tissue was undertaken according to the slow-freezing protocol, as previously described [16]. Frozen ovarian tissue was thawed at room temperature for 2 min, immersed in a water bath at 37 °C for 2 min, and then washed three times in fresh HEPES-minimal essential medium (HEPES-MEM) (Gibco) to remove the cryoprotectant [17].

One or 2 cryovials containing ovarian tissue from each patient were thawed in order to obtain 3 fragments, one measuring approximately $10\times5\times1$ mm^3 to be processed for follicle isolation, one of around $5\times5\times1$ mm^3 to be fixed in 4% formaldehyde and embedded in paraffin, and one of about $2\times2\times1$ mm^3 to be fixed in Karnovsky solution.

Follicle isolation

Primordial-primary follicles were isolated from human frozen-thawed biopsies according to the protocol used in our laboratory [18–20]. Briefly, ovarian tissue fragments were mechanically minced with a tissue chopper (McIlwain Tissue Chopper, Mickle Laboratory, Guildford, UK) and incubated in 10 mL Dulbecco's phosphate-buffered saline (PBS) with Ca2 + and Mg2 + (Gibco, Thermo Fisher Scientific, Ghent, Belgium) in the presence of 0.28 Wünsch units/mL Liberase DH (Roche Diagnostics, Brussels, Belgium) and 8 Kunitz units/mL DNase I (Roche Diagnostics, Brussels, Belgium) in a gently shaking water bath (37 °C) for 30 min and pipetted every 15 min. After 30 min, the suspension was first filtered with a cell strainer of 70 µm (Falcon, New York, USA), and then 30 µm (pluriSelect Life Science, Leipzig, Germany), before being inactivated with the same volume of PBS + 10% heat-inactivated fetal bovine serum (HIFBS). The enzymatic digestion step was repeated with ovarian tissue fragments retrieved from the 70-µm cell strainer, while isolated follicles from the 30-µm filter were recovered by washing the nylon mesh in 3 mL PBS + 10% HIFBS. Fully isolated follicles were collected with the help of a stereomicroscope and 130-µm micropipette by two operators. Filtration and follicle recovery steps were repeated on non-digested ovarian tissue fragments after 30, 60, and 90 min of enzymatic digestion and, with virtually all the fragments totally dissociated, the isolation procedure was halted. According to the differences in the composition of ovarian stroma in prepubertal ovaries [21], which shows an age-adjusted increase in collagen and decrease in hyaluronan [22], the follicle isolation protocol was adapted for prepubertal ovarian tissue. Indeed, in a previous study, Soares digested ovarian tissue from a 4-year-old girl and, after 40 min, it was overdigested [23]. For this reason, we decided to shorten the incubation time with enzymes to just 20 min, with pipetting every 10 min.

Follicle viability

To assess follicle viability, follicles were incubated in 50 µL PBS containing 2 µmol/L calcein AM and 5 µmol/L ethidium homodimer-I (LIVE/DEAD® Viability/Cytotoxicity Kit, Molecular Probes, Leyden, the Netherlands) for 30 min

at 37 °C in the dark [16]. The follicles were then classified into four categories (V1 to V4) depending on the percentage of dead granulosa cells (GCs): (V1) follicles with all GCs viable; (V2) follicles with less than 10% dead GCs; (V3) follicles with 10–50% dead GCs; and (V4) follicles with more than 50% dead GCs and/or a dead oocyte. V1 and V2 were considered to be live follicles, while V3 and V4 were classified as dead [16, 23].

Mitochondrial activity

Mitochondrial activity in isolated follicles was assessed using two fluorescent probes: MitoTracker Red CM-H2XRos (Molecular Probes, Inc., Eugene, OR, USA) and 5,5′,6,6′-tetrachloro-1,1′,3,3′-tetraethylbenzimidazolylcarbocyanine iodide (JC-1; Invitrogen, Paisley, UK). MitoTracker is a mitochondria-specific fluorescent and cell-permeant probe. It is a derivative of dihydrorhodamine and is selectively sequestered only in mitochondria with active ΔΨm, depending on their oxidative activity [24]. JC-1, on the other hand, differentially fluoresces according to ΔΨm. After entering the mitochondria, it changes color from green when present in its monomeric form (inactive mitochondria), to red as the mitochondrial membrane becomes polarized and aggregates of JC-1 form (active mitochondria). By measuring the ratio of green to red, it is possible to obtain a semi-quantitative assessment of mitochondrial polarization states [25–27].

Follicles isolated from each patient were divided into two groups. One group was incubated in 500 nM MitoTracker in Eagle's MEM (stock solution: 100 µM in dimethyl sulfoxide [DMSO]) for 30 min at 37 °C (Fig. 1A); follicles were then washed in PBS, incubated again for 60 min in 2.5% glutaraldehyde, and finally incubated in Hoechst 33,342 (1:2000 in PBS) to stain nuclei (Fig. 1B). The other group was assigned to JC-1 (1 µg/mL) in Hank's buffered saline solution (HBSS) containing 0.01% DMSO for 30 min at 37 °C [28], before being washed twice in fresh PBS (Fig. 1C and D). Follicles from both groups were collected in separate channels of a µ-Slide VI – Flat (IBIDI, Germany) and kept in the dark at 4 °C until evaluation. A Zeiss Cell Observer Spinning Disk confocal microscope with z-stacking was used for mitochondrial analysis. Microscope adjustments and photomultiplier settings were kept constant for all experiments, and background fluorescence values were subtracted. Images were acquired for each follicle as a whole unit (oocyte and surrounding GCs). MitoTracker staining was detected with a red filter (wavelength 579–599 nm), while JC-1 monomers and aggregates were respectively identified with a green filter (wavelength 520–527 nm) and a red filter (wavelength 579–599 nm).

To evaluate fluorescence intensity quantitatively in confocal microscopic sections, image analysis was performed using the ImageJ software (V1.43u; National Institutes of Health; 29). Mean staining intensity with MitoTracker was expressed in arbitrary units (mean ± SEM) [24], while the ratio of inactive/active mitochondria was obtained JC-1 and co-quantifying intensities of green (inactive mitochondria) and red (active mitochondria) fluorescence [25, 26].

Immunohistochemistry: TOMM20 analysis

After fixation in 4% formaldehyde, frozen-thawed ovarian tissue from adult and prepubertal patients was embedded in paraffin and serially sectioned (5-µm-thick sections) for immunohistochemical analysis.

Mitochondrial content was evaluated by immunostaining for TOMM20, a peptide receptor located on the surface of the outer mitochondrial membrane. Sections were first deparaffinized with Histosafe (Yvsolab SA, Beerse, Belgium) and rehydrated in 2-propanol (Merck, Darmstadt, Germany). After blocking endogenous peroxidase activity by incubation in 3% H2O2 (Merck, Darmstadt, Germany) for 30 min at room temperature, and heat epitope retrieval in citrate buffer for 75 min at 98 °C, nonspecific staining was blocked by incubation with goat serum for 30 min. The slides were incubated overnight at 4 °C with primary antibody, namely, rabbit anti-human TOMM20 (dilution 1:500, PAS-52843, Invitrogen), followed by a further 60 min at room temperature with EnVision anti-rabbit secondary antibody (Dako, North Carolina). Diaminobenzidine (DAB vector 4100, Dako, North Carolina) was used as a chromogen and nuclei were counterstained with hematoxylin. Negative controls were performed in line with current guidelines, using the rabbit-specific polyclonal antibody FLEX (ready to use, IS600, Dako, North Carolina) to substitute the primary antibody [29].

Comprehensive images of TOMM20 sections were obtained with the Leica SCN400 slide scanner at × 40 magnification (Leica Biosystems, Dublin). Follicles were delineated and annotated as a whole unit, meaning that both the oocyte and surrounding GCs were analyzed. Computer-assisted quantification of staining concentrations was achieved with Leica's proprietary artificial intelligence (TissueIA, Wetzlar, Germany) by applying the following formula: $\text{Staining intensity} = \left[\left(\left(\frac{I_A}{I_{\text{mean}}}\right) \times \left(\frac{S_{\text{posA}}}{S_{\text{posTot}}}\right)\right) + \left(\left(\frac{I_B}{I_{\text{mean}}}\right) \times \left(\frac{S_{\text{posB}}}{S_{\text{posTot}}}\right)\right) + \ldots\right] \times I_{\text{mean}}$ (where I_A = average intensity annotation A; I_{mean} = mean of average staining intensities of all annotations; S_{posA} = total tissue area of annotation A; S_{posTot} = sum of total tissue area of all annotations) [30].

Transmission electron microscopy

For ultrastructural analysis, ovarian tissue from each patient was fixed in Karnovsky solution (2% paraformaldehyde, 2.5% glutaraldehyde and 0.1 M sodium

cacodylate buffer, pH 7.2) for 24 h. After fixation, the samples were washed in sodium cacodylate buffer and postfixed in 1% osmium tetroxide for 2 h. They were rinsed again and dehydrated through an ascending series of ethanol, before being embedded in epoxy resin (Agar Scientific, Essex, UK). Resin blocks were then sectioned using an Ultracut E ultramicrotome (Reichert-Jung, Vienna, Austria). Semithin Sects. (3-µm thick) were stained with toluidine blue and examined by light microscopy (Zeiss Axioskop, Germany). Thereafter, ultrathin Sects. (50–60 nm) were obtained using a diamond knife, mounted on copper grids, and contrasted with saturated uranyl acetate and lead citrate. They were examined and photographed with a Zeiss EM10 electron microscope operating at 80 kV (Zeiss, Germany).

For transmission electron microscopy (TEM) evaluation, the morphological characteristics of the stroma, GCs, and oocytes, as well as their organelles, basal and plasmatic membranes and nuclear envelope, were taken into account. Shape, morphology, distribution, and the electron density of chromatin were also investigated.

Statistics

GraphPad Prism, version 8.1.2 for Windows (GraphPad Software, USA), was used for statistical analyses. To evaluate follicle viability, mean fluorescence intensity for both fluorescent dyes, and TOMM20 staining concentrations, the unpaired *t* test was applied to compare prepubertal and adult patients. A p value < 0.05 was considered statistically significant.

Results

Results of follicle isolation per patient are reported in Table 1. Follicles were isolated from all prepubertal ($n = 164$) and adult patients ($n = 144$). Among those recovered from prepubertal patients, 40 were analyzed for follicle viability, 62 were incubated with MitoTracker, and 62 with JC-1. In adult patients, of the 144 recovered follicles, 20 were analyzed for follicle viability, 62 were incubated with MitoTracker, and 62 with JC-1.

Follicle viability

The percentage of viable and minimally damaged follicles (V1 and V2) was lower in prepubertal follicles (54.1% vs 100% in adult follicles), albeit not significantly, while the percentage of damaged and dead follicles (V3 and V4) was significantly higher in prepubertal follicles compared to adult follicles (45.8% vs 0% respectively; $p = 0.04$).

Mitochondrial activity

The mean fluorescence intensity of mitochondrial activity calculated using the ImageJ software is summarized in Fig. 1. Mean fluorescence intensity with MitoTracker (Fig. 1E) was significantly higher in prepubertal follicles than adult follicles (mean ± SEM: 8397 ± 1515 vs 4243 ± 734.9 respectively, $p = 0.03$). Figure 1F shows the

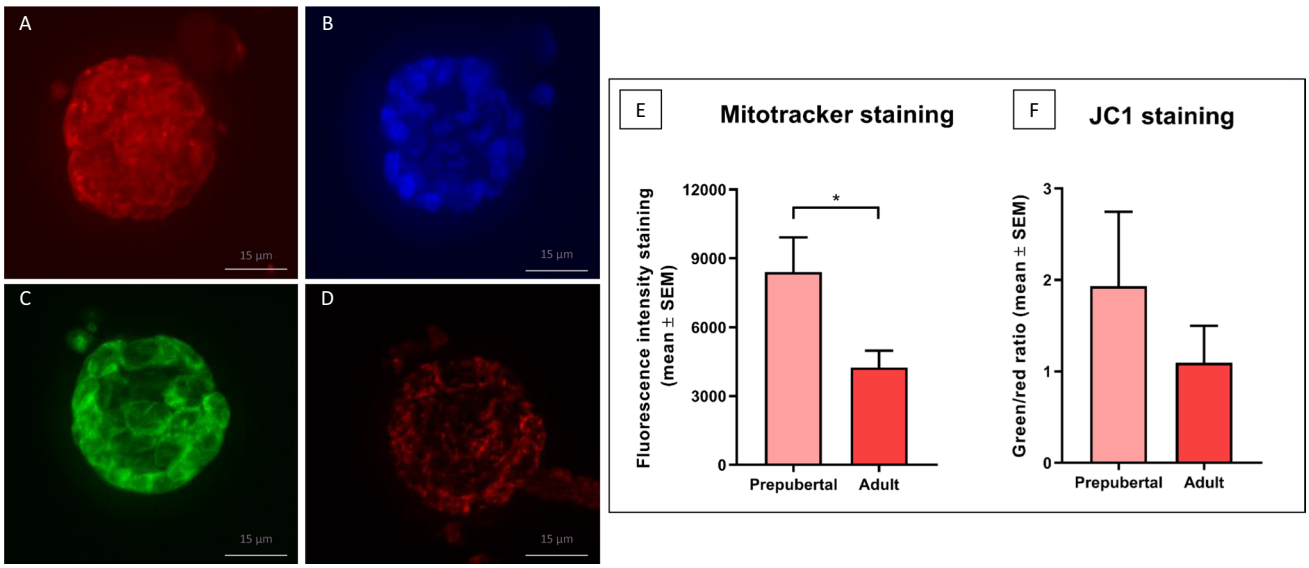

Fig. 1 Primordial-primary follicles isolated from frozen-thawed prepubertal ovarian tissue and stained with MitoTracker Red CM-H2Xros (**A**), Hoechst (**B**), and JC-1 (**C**: green detection, **D**: red detection). Mitochondrial activity was evaluated by mean fluorescence intensity expressed as arbitrary values (mean + SEM), $p = 0.03$ (**E**), while JC-1 analysis recorded as the inactive/active ratio (mean + SEM) (**F**)

Table 1 Results of follicle isolation per patient

Prepubertal group (age in years)	Number of follicles analyzed with MitoTracker	Number of follicles analyzed with JC-1	Number of follicles analyzed for viability tests (results)
Patient 1 (9)	4	4	4 (1 V1, 3 V4)
Patient 2 (3)	7	7	5 (5 V4)
Patient 3 (10)	15	12	4 (2 V1, 1 V2, 1 V3)
Patient 4 (1)	6	8	8 (4 V1, 4 V2)
Patient 5 (3)	6	13	6 (1 V1, 3 V2, 2 V3)
Patient 6 (7)	15	14	7 (2 V2, 5 V4)
Patient 7 (3)	9	4	6 (2 V1, 3 V2, 1 V3)
Total	62	62	40
Adult group (age in years)	**Number of follicles analyzed with MitoTracker**	**Number of follicles analyzed with JC-1**	**Number of follicles analyzed for viability tests (results)**
Patient 1 (29)	16	22	5 (4 V1, 1 V2)
Patient 2 (35)	7	7	0
Patient 3 (35)	7	1	0
Patient 4 (27)	7	9	8 (6 V1, 2 V2)
Patient 5 (21)	15	15	7 (5 V1, 2 V2)
Patient 6 (20)	10	8	0
Total	62	62	20

V1, follicles with all GCs viable; *V2*, follicles with less than 10% dead GCs; *V3*, follicles with 10–50% dead GCs; *V4*, follicles with more than 50% dead GCs and/or a dead oocyte

JC-1 ratio of inactive/active mitochondria, recording a ratio of 1.9 in prepubertal follicles and 1.01 in adult follicles. A high ratio value points to a large proportion of mitochondria with low $\Delta\Psi m$ and therefore low activity, while a low value indicates a small proportion of inactive mitochondria and hence a high proportion of active mitochondria.

TOMM20 analysis

TOMM20 is a mitochondrial protein present on the outer membrane and is extensively used as a marker of mitochondrial content. Staining for TOMM20 was detected in oocytes and GCs of follicles at each stage (Fig. 2A). Only follicles with a visible oocyte nucleus in the central area were investigated. A total of 278 follicles were analyzed after classification into primordial and primary stages, and pooled. A mean number of 34 follicles per patient were analyzed in the prepubertal group (Fig. 2A) and a mean of 12 in the adult group (Fig. 2B). Quantification of TOMM20, based on the intensity and extent of the signal, revealed significantly stronger TOMM20 staining in prepubertal preantral follicles than adult follicles (449.2 ± 84.25 vs 199.5 ± 32.83 respectively, $p = 0.01$) (Fig. 2C).

Transmission electron microscopy

Around 100 healthy-looking follicles from prepubertal subjects and 30 follicles from adult patients were investigated by TEM. Characteristics observed by TEM are reported in Table 2. In both groups, follicles were either at the primordial or primary stage and composed of an oocyte surrounded by a single layer of flattened or cuboidal GCs respectively. The shape of GCs was the only difference noted between primordial and primary follicles, while the ultrastructure of oocytes in primordial and primary follicles was comparable.

Upon analysis of healthy-looking follicles from adult and prepubertal tissue, GCs exhibited a similar ultrastructural aspect (Figs. 3A and 4A). They showed a large indented nucleus with compacted chromatin and free ribosomes, elements of rough and smooth endoplasmic reticulum, scattered vacuoles, and mitochondria dispersed throughout the cytoplasm. Mitochondria in GCs were mostly rod-shaped and contained regular transverse cristae, with no visible difference between prepubertal and adult patients.

On the other hand, oocytes from adult follicles showed some differences compared to oocytes from prepubertal samples. In adult oocytes, a large, spherical nucleus was surrounded by cytoplasmic organelles, constituting Balbiani's vitelline body (Fig. 4A). In all adult oocytes, mitochondria were mostly round in shape (Fig. 4B), with a pale matrix and peripheral archiform cristae (Fig. 4C), and were closely associated with the nucleus, forming the paranuclear complex [31].

In prepubertal follicles, mitochondria in oocytes were heterogeneously dispersed throughout the cytoplasm in clusters, and separate clusters were identified, as shown in Fig. 3A. Unlike in adult oocytes, Balbiani's vitelline body

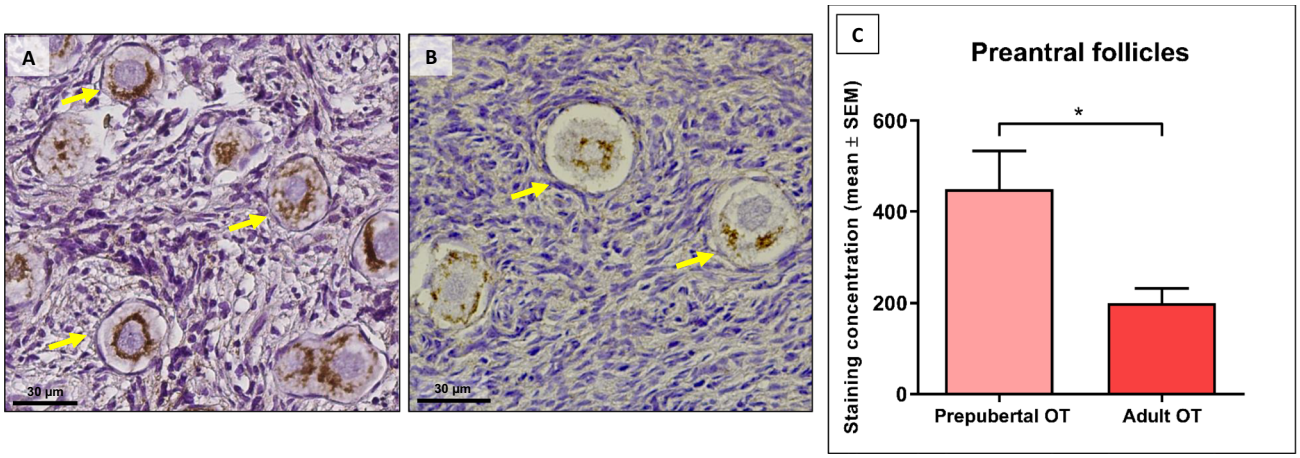

Fig. 2 **A-B**: TOMM-20 immunostaining in prepubertal (**A**) and adult (**B**) ovarian tissue showing primordial follicles. Cytoplasmic staining is visible around the oocyte nucleus showing (arrows). **C** TOMM20 staining concentrations in prepubertal and adult ovarian tissue (mean + SEM). $p = 0.01$. OT: ovarian tissue

was not clearly visible. Most mitochondria in prepubertal oocytes have a dense matrix and an irregular morphology. They were either round or elongated in shape, with large longitudinal as opposed to small archiform cristae (Fig. 3B). Some mitochondria exhibited cristae shaped in the form of a fingerprint (Fig. 3C).

Discussion

Ovarian tissue cryopreservation and transplantation is currently the only available fertility preservation option for prepubertal patients [2], but the ability of prepubertal follicles to grow and mature adequately after freezing and grafting still needs to be evaluated. Transplantation of ovarian tissue cryopreserved before puberty has been performed in three patients to date. Evidence of puberty induction was reported in two of these cases [32, 33], and a live birth of a healthy baby was recently achieved [3].

Ovarian tissue from prepubertal patients shows differences with its adult counterpart [4–6], but the source of this difference is still unknown, which is why mitochondria have been extensively investigated in animal and human oocytes [15, 24, 27, 34–36]. During oogenesis, important modifications occur, both in terms of mitochondrial number and transcripts, and rearrangement and maturation [15, 24, 27, 34–36]. These phenomena appear to be a prerequisite for acquisition of developmental competence [37]. Advancing maternal age results in the gradual decline of oocyte quality and developmental potential [38]. This age-related dysfunction is usually attributable to increased oxidative stress and accumulation of free radicals within mitochondria, which ultimately results in mtDNA mutations and a consequent drop in ATP production, cell cycle arrest, and apoptosis [39–42]. Despite being well known for their primary function in oocyte developmental capacity and embryo development [7, 11–14], our understanding of mitochondria in prepubertal ovarian tissue is still somewhat lacking.

In the present study, we evidenced differences in the number of mitochondria between human prepubertal and adult follicles. Quantification of TOMM20 staining intensity revealed higher mitochondrial content in prepubertal follicles than adult follicles. In 2001, Pepling and Spradling reported that in fetal mouse ovaries, mitochondria multiply very quickly and reorganize themselves in primordial germ cells prior to germ cell nest breakdown [43]. A few years later, Tingen et al. proposed that some germ cells might act as "nurse cells," whose fate is to provide nutrients and

Table 2 Characteristics observed by TEM

	Prepubertal follicles	Adult follicles
GCs	no difference	no difference
Oocyte nucleus	Absence of Balbiani's vitelline body	Balbiani's vitelline body
Mitochondria organization	Clusters, heterogeneously dispersed	Closely associated to the nucleus
Mitochondria shape	Elongated	Round
Mitochondria cristae	Longitudinal or fingerprint	Peripheral and archiform
Mitochondria matrix	Dense	Pale

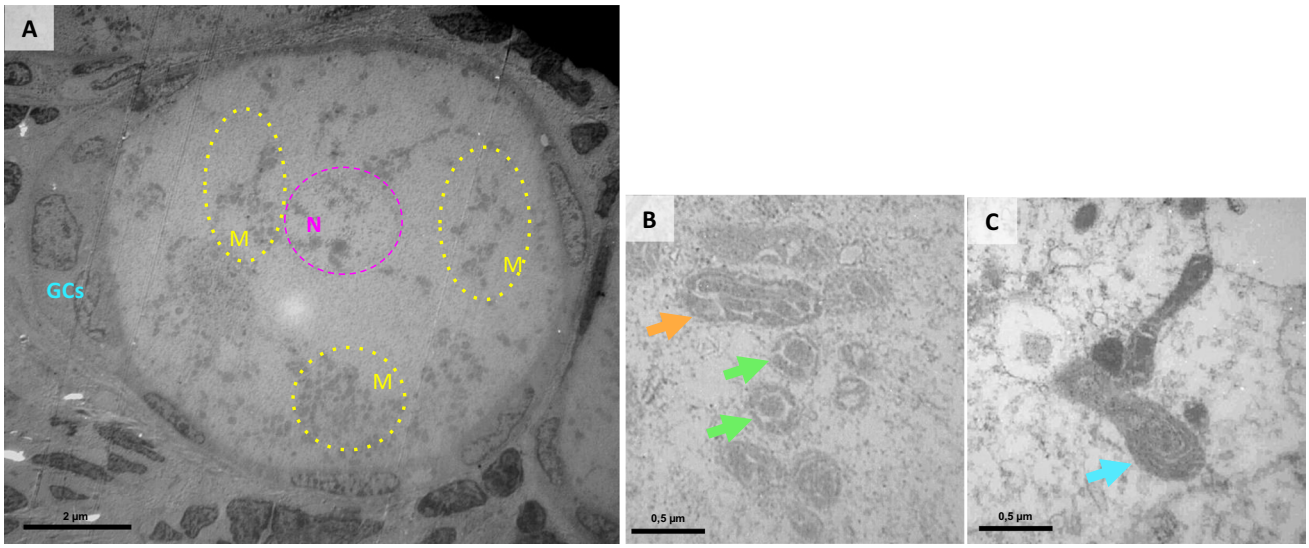

Fig. 3 **A** intermediate follicle from a prepubertal patient exhibiting widespread mitochondrial clusters (yellow circles) surrounding the oocyte nucleus (pink circle). **B** mitochondria with longitudinal and irregular cristae shown in a sagittal (arrow head) and transverse section (arrows). **C** mitochondria with fingerprint-like cristae (arrow). N: oocyte nucleus, GCs: granulosa cells, M: mitochondria

cellular organelles such as mitochondria to other follicles, which are instead selected to survive [44]. A consequence of energy generation in mitochondria is ROS production and mtDNA mutations, which are potentially harmful and able to cause premature deterioration of oocytes [45, 46]. As females are born with a finite number of ovarian follicles that do not regenerate during life, avoidance of accumulating mtDNA mutations is vital to preserving the quality of oocytes throughout the reproductive lifespan. We might therefore hypothesize that a scrupulous process of selection is fundamental to eliminating damaged or dysfunctional mitochondria and only allowing survival of those that are healthy and properly functioning. Hence, even though the total number of mitochondria is reduced in adulthood, adult ovarian follicles carry only functional mitochondria.

Fluorescent intensity measurement of MitoTracker-labeled mitochondria revealed greater activity in prepubertal than adult follicles. As previously stated, the number of mitochondria in prepubertal follicles is also higher, so we might conclude that the greater mitochondrial activity detected by the MitoTracker could well be the consequence of higher numbers of mitochondria present in prepubertal follicles. On the whole, prepubertal follicles appear to be markedly more active than adult follicles.

Interestingly, fluorescence intensity measurement of JC-1-stained mitochondria showed that the inactive/active ratio was almost double in prepubertal compared to adult follicles,

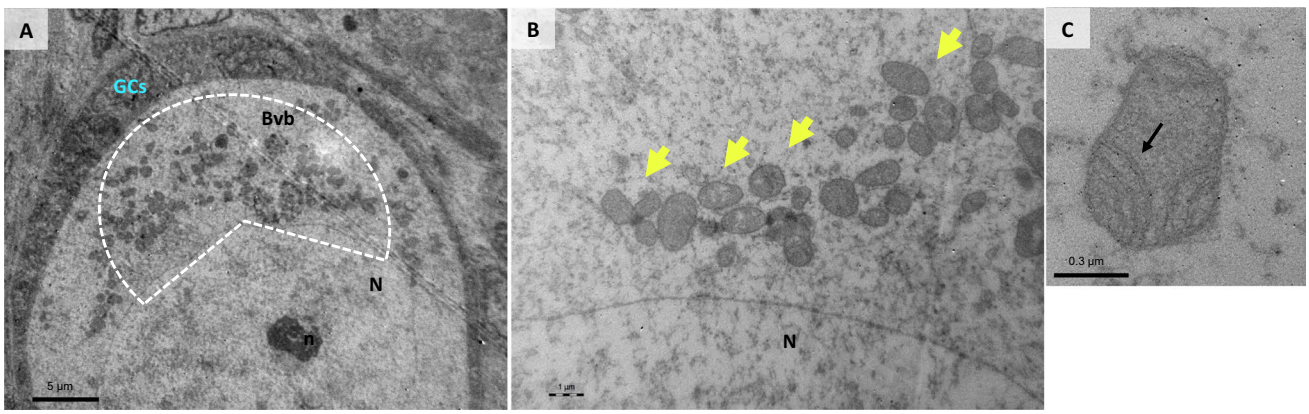

Fig. 4 **A** intermediate follicle from adult patient showing the Balbiani's vitelline body. **B** mitochondria surrounding the oocyte nucleus (yellow arrows). **C** mitochondria with arciform cristae (arrow). N: oocyte nucleus, n: nucleolus; GCs: granulosa cells, M: mitochondria

suggesting the presence of a proportion of inactive or dysfunctional mitochondria in the prepubertal group. The lower inactive/active ratio in adults could be the result of a drop in inactive mitochondria numbers. This hypothesis further supports the theory of a selection process that takes place in ovarian follicle mitochondria throughout childhood. In this instance, elimination of non-functioning and dysfunctional mitochondria leads to a reduction in the total number of mitochondria and survival of mitochondria with improved functionality in adult follicles, as corroborated by TOMM20 and MitoTracker results, respectively.

Our hypothesis is further strengthened by our ultrastructural analysis by TEM. In the prepubertal group, mitochondria appeared to be more heterogeneous than adult mitochondria. The majority were elongated in shape and showed a peculiar arrangement and shape of their cristae. In fact, in prepubertal follicles, some mitochondrial cristae looked enlarged and mostly longitudinally oriented, delimiting irregular intermembrane and intercristae spaces, while others resembled fingerprints. Moreover, the matrices of prepubertal mitochondria appeared to be more dense than those of adults, suggesting a higher density of cristae.

Mitochondria are extremely dynamic organelles and changes in mitochondrial morphology help them adapt to specific cellular and tissue demands [47]. Indeed, mitochondrial morphology reflects changes in the energetic state of mitochondria [48], and the shape of mitochondrial cristae regulates respiratory chain supercomplex stability and assembly [49]. An intriguing explanation for these findings could be linked to their autophagic degradation. Interestingly, during autophagy, mitochondria undergo a series of morphological changes, causing them to elongate and the number of cristae per surface area to increase. Dimerization of ATP synthase is then enhanced, leading to optimized ATP production [50]. These changes not only allow mitochondria to be spared from autophagic degradation but also to sustain ATP production, which is fundamental to the process of autophagy [51]. Some studies in animal models have reported that autophagy might be the cell death mechanism governing maintenance of quiescence of the follicle pool and elimination of non-viable prepubertal follicles [52]. Our results may support this theory; indeed, autophagy could be the mechanism by which inactive or dysfunctional mitochondria are removed, while ultrastructural changes observed in prepubertal mitochondria might well be the response of functional mitochondria to escape autophagic degradation.

Before making any definitive claims, we must consider the outcomes of viability tests. In fact, the percentage of non-viable follicles was found to be higher in the prepubertal group than in the adult group, in line with our previous work [6]. Detection of more V3 and V4 follicles in prepubertal patients compared to adult subjects is due to the process of physiological elimination of follicles that occurs during childhood. We actually hypothesized that there is a process of elimination whereby deficient follicles act as a source of cytoplasmic and nuclear material for healthy and viable follicles [6].

Conclusion

In conclusion, this is the first study to characterize mitochondria in prepubertal follicles. Prepubertal follicles contain more mitochondria and, because of these higher numbers, they are generally more active than adult follicles. Nevertheless, in prepubertal patients, there is also a proportion of inactive or dysfunctional mitochondria, which decreases considerably by adulthood. These results clearly point to a process of selection and maturation of immature mitochondria during childhood, with either elimination or transformation of inactive or dysfunctional mitochondria in order to preserve only mature and properly functioning mitochondria inside adult follicles. We also evidenced differences in the ultrastructure of prepubertal mitochondria. These structural differences might be the way in which functioning mitochondria respond to the autophagic process responsible for elimination of inactive or dysfunctional mitochondria. Taken together, these results suggest that prepubertal mitochondria may be immature compared to their adult counterparts, and that changes to their morphology and functional state are required in order to reach adulthood.

Acknowledgements The authors thank Mira Hryniuk, B.A., for reviewing the English language of the article, and Dolores Gonzalez, Olivier Van Kerk, and Sarah Storder for their technical assistance.

Author contribution R.M.: conception and design of the study, experimental procedures, analysis of results, statistical analysis, and article preparation; M.C.C.: experimental procedures, analysis of results and discussion contribution; A.C.: experimental procedures, data evaluation, and discussion contribution; C.A.A.: discussion contribution; J.D.: data evaluation, discussion contribution, and article revision; M.M.D.: conception and design of the study, data evaluation, discussion contribution, and article revision.

Funding This study was supported by grants from the Fonds National de la Recherche Scientifique de Belgique (FNRS-PDR Convention T.0077.14, Télévie grant 7.4590.16 awarded to Rossella Masciangelo, EOS grant 30443682 to Maria Costanza Chiti, and 5/4/150/5 grant to Marie-Madeleine Dolmans; CAA is an FSR-FNRS research associate), and the Foundation Against Cancer (grant 2018–042 awarded to Alessandra Camboni).

Declarations

Competing interests The authors declare no competing interests.

References

1. Donnez J, Dolmans MM. Fertility Preservation in Women. N Engl J Med. 2017;377(17):1657–65.
2. Wallace WH, Anderson RA, Irvine DS. Fertility preservation for young patients with cancer: who is at risk and what can be offered? Lancet Oncol. 2015;6:209–18.
3. Matthews SJ, Picton H, Ernst E, Andersen CY. Successful pregnancy in a woman previously suffering from β-thalassemia following transplantation of ovarian tissue cryopreserved before puberty. Minerva Ginecol. 2018;70:432–5.
4. Luyckx V, Scalercio S, Jadoul P. Evaluation of cryopreserved ovarian tissue from prepubertal patients after long-term xenografting and exogenous stimulation. Fertil Steril. 2013;100(5):1350–7.
5. Anderson RA, McLaughlin M, Wallace WH, Albertini DF, Telfer EE. The immature human ovary shows loss of abnormal follicles and increasing follicle developmental competence through childhood and adolescence. Hum Reprod. 2014;29(1):97–106.
6. Masciangelo R, Chiti MC, Philippart C, Amorim CA, Donnez J, Camboni A, Dolmans MM. Follicle populations and vascularization in ovarian tissue of pediatric patients before and after long-term grafting. Fertil Steril. 2020;114(6):1330–8.
7. Zou W, Slone J, Cao Y, Huang T. Mitochondria and their role in human reproduction. DNA Cell Biol. 2020;39(8):1370–8.
8. Zorova LD, Popkov VA, Plotnikov EY. Mitochondrial membrane potential. Anal Biochem. 2018;552:50–9.
9. Van Blerkom J. Mitochondrial function in the human oocyte and embryo and their role in developmental competence. Mitochondrion. 2011;11(5):797–813.
10. Santos TA, El Shourbagy S, St John JC. Mitochondrial content reflects oocyte variability and fertilization outcome. Fertil Steril. 2006;85(3):584–91.
11. Stojkovic M, Machado SA, Stojkovic P. Mitochondrial distribution and adenosine triphosphate content of bovine oocytes before and after in vitro maturation: correlation with morphological criteria and developmental capacity after in vitro fertilization and culture. Biol Reprod. 2001;64(3):904–9.
12. Wilding M, Dale B, Marino M. Mitochondrial aggregation patterns and activity in human oocytes and preimplantation embryos. Hum Reprod. 2001;16(5):909–17.
13. Nagano M, Katagiri S, Takahashi Y. ATP content and maturational/developmental ability of bovine oocytes with various cytoplasmic morphologies. Zygote. 2006;14(4):299–304.
14. Cozzolino M, Marin D, Sisti G. New Frontiers in IVF: mtDNA and autologous germline mitochondrial energy transfer. Reprod Biol Endocrinol. 2019;17(1):55.
15. May-Panloup P, Boucret L, Chao de la Barca JM. Ovarian ageing: the role of mitochondria in oocytes and follicles. Hum Reprod Update. 2016;22(6):725–43.
16. Gosden RG, Baird DT, Wade JC, Webb R. Restoration of fertility to oophorectomized sheep by ovarian autografts stored at -196 degrees C. Hum Reprod. 1994;9:597–603.
17. Amorim CA, Dolmans MM, David A. Vitrification and xenografting of human ovarian tissue. Fertil Steril. 2012;98(5):1291–8.
18. Dolmans MM, Michaux N, Camboni A, Martinez-Madrid B, Van Langendonckt A, Nottola SA, et al. Evaluation of Liberase, a purified enzyme blend, for the isolation of human primordial and primary ovarian follicles. Hum reprod. 2006;21(2):413–20.
19. Vanacker J, Camboni A, Dath C, Van Langendonckt A, Dolmans MM, Donnez J, et al. Enzymatic isolation of human primordial and primary ovarian follicles with Liberase DH: protocol for application in a clinical setting. Fertil Steril. 2011;96(2):379–83.
20. Chiti MC, Dolmans MM, Hobeika M, Cernogoraz A, Donnez J, Amorim CA. A modified and tailored human follicle isolation procedure improves follicle recovery and survival. J Ovarian Res. 2017;10(1):71.
21. Ouni E, Bouzin C, Dolmans MM, Marbaix E, PyrDit Ruys S, Vertommen D, Amorim CA. Spatiotemporal changes in mechanical matrisome components of the human ovary from prepuberty to menopause. Hum Reprod. 2020;35(6):1391–410.
22. Amargant F, Manuel SL, Tu Q, Parkes WS, Rivas F, Zhou LT, et al. Ovarian stiffness increases with age in the mammalian ovary and depends on collagen and hyaluronan matrices. Aging Cell. 2020;19(11):e13259.
23. Soares M, Saussoy P, Maskens M. Eliminating malignant cells from cryopreserved ovarian tissue is possible in leukaemia patients. Br J Haematol. 2017;178(2):231–9.
24. Leoni GG, Palmerini MG, Satta V. Differences in the kinetic of the first meiotic division and in active mitochondrial distribution between prepubertal and adult oocytes mirror differences in their developmental competence in a sheep model. Plos One. 2015;10(4):e0124911.
25. Harris SE, Maruthini D, Tang T, Balen AH, Picton HM. Metabolism and karyotype analysis of oocytes from patients with polycystic ovary syndrome. Hum Reprod. 2010;25:2305–15.
26. Picton HM, Elder K, Houghton FD. Association between amino acid turnover and chromosome aneuploidy during human preimplantation embryo development in vitro. Mol Human Reprod. 2010;16:557–69.
27. Cotterill M, Harris SE, Collado FE. The activity and copy number of mitochondrial DNA in ovine oocytes throughout oogenesis in vivo and during oocyte maturation in vitro. Mol Hum Reprod. 2013;19(7):444–50.
28. Van Blerkom J, Davis P, Alexander S. Inner mitochondrial membrane potential (DeltaPsim), cytoplasmic ATP content and free Ca2+ levels in metaphase II mouse oocytes. Hum Reprod. 2003;18(11):2429–40.
29. Hewitt SM, Baskin DG, Frevert CW, Stahl WL, Rosa-Molinar E. Controls for immunohistochemistry: the Histochemical Society's standards of practice for validation of immunohistochemical assays. J Histochem Cytochem. 2014;62(10):693–7.
30. Courtoy GE, Donnez J, Marbaix E, Barreira M, Luyckx M, Dolmans MM. Progesterone receptor isoforms, nuclear corepressor-1 and steroid receptor coactivator-1 and b-cell lymphoma 2 and Akt and Akt phosphorylation status in uterine myomas after ulipristal acetate treatment: a systematic immunohistochemical evaluation. Gynecol Obstet Invest. 2018;83:443–54.
31. Nottola SA, Camboni A, Van Langendonckt A. Cryopreservation and xenotransplantation of human ovarian tissue: an ultrastructural study. Fertil Steril. 2008;90(1):23–32.
32. Poirot C, Abirached F, Prades M, Coussieu C, Bernaudin F, Piver P. Induction of puberty by autograft of cryopreserved ovarian tissue. Lancet. 2012;379:588.
33. Ernst E, Kjaersgaard M, Birkebaek NH, Clausen N, Andersen CY. Case report: stimulation of puberty in a girl with chemo- and radiation therapy induced ovarian failure by transplantation of a small part of her frozen/thawed ovarian tissue. Eur J Cancer. 2013;49:911–4.
34. Bachvarova R. Gene expression during oogenesis and oocyte development in mammals. Dev Biol. 1985;1:453–524.
35. De La Fuente R, Viveiros MM, Burns KH, Adashi EY, Matzuk MM, Eppig JJ. Major chromatin remodeling in the germinal vesicle (GV) of mammalian oocytes is dispensable for global transcriptional silencing but required for centromeric heterochromatin function. Dev Biol. 2004;275:447–58.
36. Sánchez F, Adriaenssens T, Romero S, Smitz J. Quantification of oocyte-specific transcripts in follicle-enclosed oocytes during antral development and maturation in vitro. Mol Hum Reprod. 2008;15(9):539–50.

37. Songsasen N, Henson LH, Tipkantha W. Dynamic changes in mitochondrial DNA, distribution and activity within cat oocytes during folliculogenesis. Reprod Domest Anim. 2017;52:71–6.
38. Zhang D, Keilty D, Zhang ZF, Chian RC. Mitochondria in oocyte aging: current understanding. Facts Views Vis Obgyn. 2017;9(1):29–38.
39. Harman D. Aging: a theory based on free radical and radiation chemistry. J Gerontol. 1956;11:298–300.
40. Trifunovic A, Wredenberg A, Falkenberg M. Premature ageing in mice expressing defective mitochondrial DNA polymerase. Nature. 2004;429:417–23.
41. Greaves LC, Beadle NE, Taylor GA. Quantification of mitochondrial DNA mutation load. Aging Cell. 2009;8:566–72.
42. Wang T, Zhang M, Jiang Z, Seli E. Mitochondrial dysfunction and ovarian aging. Am J Reprod Immunol. 2017;77(5).
43. Pepling ME, Spradling AC. Mouse ovarian germ cell cysts undergo programmed breakdown to form primordial follicles. Dev Biol. 2001;234(2):339–51.
44. Tingen C, Kim A, Woodruff TK. The primordial pool of follicles and nest breakdown in mammalian ovaries. Mol Hum Reprod. 2009;15(12):795–803.
45. Faron J, Bernaś T, Sas-Nowosielska H, Klag J. Analysis of the behavior of mitochondria in the ovaries of the earthworm Dendrobaena veneta Rosa 1839. PLoS One. 2015;10(2):e0117187.
46. Chen H, Chan DC. Mitochondrial dynamics in regulating the unique phenotypes of cancer and stem cells. Cell Metab. 2017;26(1):39–48.
47. Giacomello M, Pyakurel A, Glytsou C, Scorrano L. The cell biology of mitochondrial membrane dynamics. Nat Rev Mol Cell Biol. 2020;21(4):204–24.
48. Galloway CA, Lee H, Yoon Y. Mitochondrial morphology-emerging role in bioenergetics. Free Radic Biol Med. 2012;53(12):2218–28.
49. Cogliati S, Frezza C, Soriano ME. Mitochondrial cristae shape determines respiratory chain supercomplexes assembly and respiratory efficiency. Cell. 2013;155(1):160–71.
50. Gomes LC, Di Benedetto G, Scorrano L. During autophagy mitochondria elongate, are spared from degradation and sustain cell viability. Nat Cell Biol. 2011;13(5):589–98.
51. Gomes LC, Scorrano L. Mitochondrial morphology in mitophagy and macroautophagy. Biochim Biophys Acta. 2013;1833(1):205–12.
52. Tingen CM, Bristol-Gould SK, Kiesewetter SE, Wellington JT, Shea L, Woodruff TK. Prepubertal primordial follicle loss in mice is not due to classical apoptotic pathways. Biol Reprod. 2009;81(1):16–25.